



ELSEVIER

Journal of Crystal Growth 226 (2001) 111–116

JOURNAL OF  
**CRYSTAL  
GROWTH**

www.elsevier.nl/locate/jcrysgr

# Growth and electrical properties of $\text{Pb}(\text{Sc}_{1/2}\text{Nb}_{1/2})\text{O}_3$ – $\text{Pb}(\text{Mg}_{1/3}\text{Nb}_{2/3})\text{O}_3$ – $\text{PbTiO}_3$ ternary single crystals by a modified Bridgman technique

Yiping Guo\*, Haiqing Xu, Haosu Luo, Guisheng Xu, Zhiwen Yin

*Laboratory of Functional Inorganic Materials, Shanghai Institute of Ceramics, Chinese Academy of Sciences,  
Shanghai 201800, People's Republic of China*

Received 5 February 2001; accepted 9 March 2001

Communicated by T.F. Kuech

## Abstract

Single crystals of  $0.05\text{Pb}(\text{Sc}_{1/2}\text{Nb}_{1/2})\text{O}_3$ – $0.63\text{Pb}(\text{Mg}_{1/3}\text{Nb}_{2/3})\text{O}_3$ – $0.32\text{PbTiO}_3$  have been grown directly from melt by a modified Bridgman technique. The crystals with perovskite structure were 15 mm in diameter and 20 mm in length. The segregation during the growth of the single crystals was studied by means of X-ray diffraction analysis. The results show that  $\text{PbTiO}_3$  content increases throughout the crystal growth. The electrical properties of the single crystals oriented along the  $[001]$  axis have been characterized. The plates cut from the seed end of a boule exhibited a permittivity ( $\epsilon_{33}/\epsilon_0$ ) of about 3500, dielectric loss tangent ( $\text{tg}\delta$ ) < 1%, dielectric constant peaks at 162°C, piezoelectric constant ( $d_{33}$ )  $\approx$  1200 pC/N, and electromechanical coupling factor ( $k_t$ )  $\approx$  60% for the thickness mode. Our results show that  $x\text{Pb}(\text{Sc}_{1/2}\text{Nb}_{1/2})\text{O}_3$ – $y\text{Pb}(\text{Mg}_{1/3}\text{Nb}_{2/3})\text{O}_3$ – $(1-x-y)\text{PbTiO}_3$  single crystals are promising for a wide range of electro-mechanical transducer applications. © 2001 Elsevier Science B.V. All rights reserved.

**Keywords:** A1. Segregation; A1. Curie temperature; A2. Growth from melt; A2. Single crystal growth; B1. Perovskites; B2. Piezoelectric materials

## 1. Introduction

Recently, much attention has been paid to single crystals of solid solutions of lead-based complex perovskite  $\text{Pb}(\text{B}_1, \text{B}_2)\text{O}_3$  ( $\text{B}_1 = \text{Mg, Zn, Ni, Fe, Sc, In}$ ;  $\text{B}_2 = \text{Nb, Ta, W}$ ) relaxor ferroelectrics and the normal ferroelectric  $\text{PbTiO}_3$  (PT) system near the morphotropic phase boundary (MPB), which

separates the rhombohedral and tetragonal phases. The materials exhibit superior piezoelectric properties by utilizing domain engineering [1–4]. For example,  $0.67\text{Pb}(\text{Mg}_{1/3}\text{Nb}_{2/3})\text{O}_3$ – $0.33\text{PbTiO}_3$  (PMNT 67/33) single crystals show an ultrahigh piezoelectric constant ( $d_{33} \sim 2500$  pC/N) and electromechanical coupling factor in the longitudinal bar mode ( $k_{33} \sim 94\%$ ) along the  $[001]$  axis in the rhombohedral phase [5]. These values are much larger than that of  $d_{33} \sim 700$  pC/N and  $k_{33} = 70$ – $80\%$  of conventional  $\text{Pb}(\text{Zr, Ti})\text{O}_3$  (PZT) ceramics [6,7], which have been widely used in

\*Corresponding author. Tel.: +86-021-3998-6059; fax: +86-021-5992-7184.

E-mail address: hsluo@public3.sta.net.cn (Y. Guo).

ultrasonic transducers and strain actuators in the past 40 years [8]. It is known that the PZT has a high  $T_C$  ranging from 200°C–350°C, but it is very difficult to grow a PZT single crystal of a sufficient size [7,9]. Although PMNT 67/33 and 0.91Pb(Zn<sub>1/3</sub>Nb<sub>2/3</sub>)O<sub>3</sub>–0.09PbTiO<sub>3</sub>(PZNT 91/9) single crystals can be grown relatively easily, these single crystals also have some disadvantages. The poor thermal stability of PZNT 91/9 perovskite structure, relatively low Curie temperature ( $T_C < 155^\circ\text{C}$ ) of PMNT 67/33 restrain them from some applications. Therefore, a new type of single crystal with higher  $T_C$  and good perovskite thermal stability is desired. 0.58Pb(Sc<sub>1/2</sub>Nb<sub>1/2</sub>)O<sub>3</sub>–0.42PbTiO<sub>3</sub>(PSNT 58/42) single crystals, grown by a flux method, which have higher  $T_C$  and good perovskite thermal stability have also been reported [10]; but it has two major shortcomings: a high melting point of 1420°C and a high cost of the raw-materials. The ternary system of  $x\text{Pb}(\text{Sc}_{1/2}\text{Nb}_{1/2})\text{O}_3$ – $y\text{Pb}(\text{Mg}_{1/3}\text{Nb}_{2/3})\text{O}_3$ – $(1-x-y)\text{PbTiO}_3$  (PSMNT 100x/100y/100z) has a great potential to meet the requirements, if single crystals of sufficient size and good quality can be grown. Excellent electromechanical coupling factors,  $k_p > 72\%$  and  $k_{33} > 77\%$ , a relatively high  $T_C$  ( $T_C = 205^\circ\text{C}$ ) and good perovskite thermal stability of PSMNT 29/34/37 ceramics near the MPB have been reported [11]. Though single crystals of PSMNT have been grown by a flux method [12], the small size restricts further investigation. Recently, we have grown larger size PSMNT single crystals by a modified Bridgman technique, and their performance has been characterized.

## 2. Experimental procedure

Single crystals of the PSMNT ternary system near the MPB were grown directly from melt by a modified Bridgman technique (Fig. 1). The selected composition was PSMNT 5/63/32 [11]. Chemicals of high purity better than 99.99%, comprising PbO, MgO, TiO<sub>2</sub>, Sc<sub>2</sub>O<sub>3</sub> and Nb<sub>2</sub>O<sub>5</sub> were used as the starting materials. A total of 40 g was put into a 40 cm<sup>3</sup> platinum crucible, and the Pt crucible was sealed to prevent the evaporation of

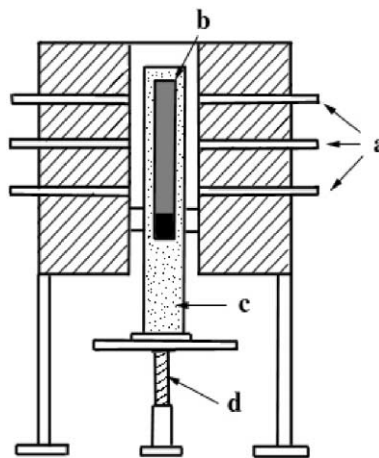


Fig. 1. Schematic diagram of the Bridgman furnace for the growth of PSMNT single crystals. (a) Heating equipments (b) Pt crucible (c) Al<sub>2</sub>O<sub>3</sub> powder (d) Drop-down mechanism.

lead. The PMNT 67/33 crystals were used as seed crystal.

The highest furnace temperature was greater than 1380°C and the temperature gradient was about 40–100°C/cm at the solid–liquid interface. The furnace temperature was regulated using a proportional integral differential (PID) controller. The growth temperature profile used was rapid heating to 1350°C, after soaking for about 10 h, the crucible was dropped at the rate of 0.1–1.0 mm/h. At the end of the growth process, the furnace temperature was cooled at the rate of 25°C/h to room temperature, crucibles were weighed to evaluate the weight loss of contents during the crystal growth.

The melting point and thermal stability of the grown crystals were measured using a simultaneous thermogravimetric analysis (TG) and differential thermal analysis (DTA). Samples were heated from 500°C to 1400°C at 10°C/min, in an argon gas atmosphere. Single crystals were ground into a fine powder for X-ray diffraction (XRD) analysis ranging from 10° to 70°(2θ), in order to confirm the phase and to calculate lattice parameters. Single crystals were orientated along the [00 1] crystallographic axis using the X-ray diffractometer.

For electrical characterization, plate samples with thickness 0.7 mm were used. Samples were

polished with  $\text{Al}_2\text{O}_3$  powders, and silver paste was painted on the crystal surfaces and fired at  $550^\circ\text{C}$  for 30 min. The specimens were immersed in silicon oil and poled in a  $10\text{ kV/cm}$  field. The electric field was applied at a temperature of  $150^\circ\text{C}$  for 15 min, and the specimens were cooled to room temperature in the field. Dielectric properties were measured using a computer controlled HP4192A impedance analyzer from room temperature to  $250^\circ\text{C}$  between 100 Hz and 10 kHz, and piezoelectric constant  $d_{33}$  was measured by a quasi-static meter of Berlincourt type at about 55 Hz. The electromechanical coupling factor  $k_t$  of thickness mode was calculated from resonance and anti-resonance frequencies.

### 3. Results and discussion

#### 3.1. Crystal structure and thermal stability

As-grown crystals were more transparent than PMNT 67/33, but sometimes possessed a few cracks. The crystal boules were 15 mm in diameter and 20 mm in length. They were light yellow in color (Fig. 2). The cracks are approximately parallel to (001) face. From the results of the phase diagram for the  $\text{Pb}(\text{B}_1, \text{B}_2)\text{O}_3\text{-PbTiO}_3$  system, there are two phase transitions near MPB composition while relaxor-PT materials are heated, rhombohedral ferroelectric (FE) phase  $\rightarrow$  tetragonal FE phase (3 m  $\rightarrow$  4 m) and tetra-

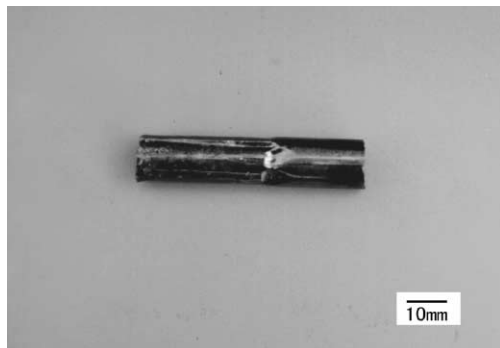


Fig. 2. As-grown PSMNT5/63/32 single crystal boule by a modified Bridgman technique.

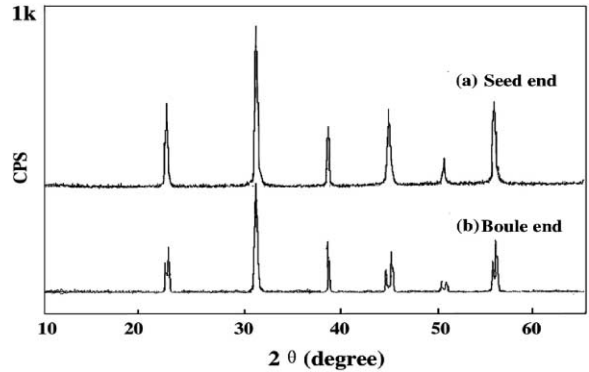


Fig. 3. X-ray diffraction (XRD) patterns for seed end (a) and boule end (b) of a PSMNT5/63/32 boule.

gonal FE phase  $\rightarrow$  cubic paraelectric (PA) phase (4 m  $\rightarrow$  m3 m). The cracks may be caused by stress brought about by the lattice deformation during phase transition and thermal gradient during crystal growth. To eliminate the cracking of the single crystals, further studies are in progress to optimize growth environments such as heating reservoir, cooling rate and so on.

The XRD analysis shows that the crystals are pyrochlore-free (Fig. 3). It also shows that the composition of the PSMNT 5/63/32 boule varies from the seed crystal. The rhombohedral (R) phase appeared at the seed end of the boule; however, the splitting of the peaks in the XRD pattern (Fig. 3(b)) would indicate a tetragonal (TR) phase at the end of the boule. For example, the fourth peak  $(200)_R$  was split into  $(200)_{TR}$  and  $(002)_{TR}$  peaks. This result shows that the  $\text{PbTiO}_3$  content increases during the growth of solid solution PSMNT single crystals due to segregation, which is similar to the growth of PMNT single crystals [13]. While PSMNT single crystals are grown directly from melt with a low growth rate, the  $\text{PbTiO}_3$  content at the seed end will be less than that in the melt. The  $\text{PbTiO}_3$  content at the boule end is greater than that at the seed end. The lattice constant is shown in Table 1. The lattice constant is close to that of the seed crystal PMNT 67/33, indicating that the PMNT 67/33 seed crystal is suitable for the growth of PSMNT 5/63/32.

Fig. 4 shows the thermal properties of one of the PSMNT single crystals investigated by TG and

Table 1  
The XRD pattern index of PSMNT single crystal

XRD pattern	Rhombohedral phase (Seed end) $a_0=4.016$		Tetragonal phase (Boule end) $a_0=4.000; c_0=4.048$	
	$hkl$	$d_{hkl}$	$hkl$	$d_{hkl}$
No.1	100	4.016	001	4.048
No.2	110	2.837	100	4.000
No.3	111	2.315	101	2.845
No.4	200	2.005	110	2.848
No.5	210	1.794	111	2.318
No.6	211	1.637	200	2.024
			200	1.999
			102	1.806
			201	1.792
			112	1.646
			211	1.636

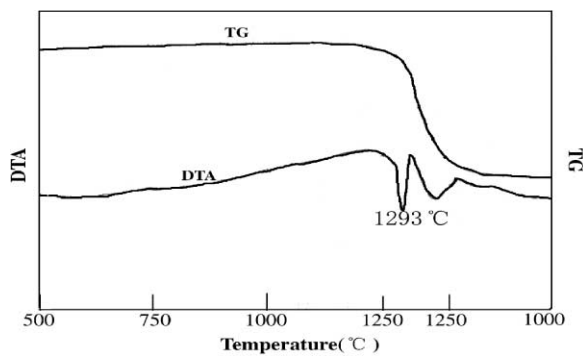


Fig. 4. A simultaneous thermogravimetric analysis (TG) and differential thermal analysis (DTA) curves for one of the PSMNT single crystals.

DTA. Upon heating, a sharper endothermic DTA peak appears at 1293°C, which corresponds to the melting of the PSMNT crystals. The TG curve indicates the high thermal stability of the PSMNT crystals without significant weight loss up to 1146°C, which indicates that PSMNT single crystals can be grown directly from melt by a Bridgman technique.

### 3.2. Electrical properties

Fig. 5(a) and (b) shows the real and imaginary parts of permittivity, as a function of temperature and frequency, for the poled (001) plates cut from

the seed end and the boule end of a boule. The dielectric constant peaks are 162°C and 180°C, respectively, indicating a  $T_C$  which almost equals to the PZNT 91/9. The figures also exhibit a frequency dispersion of the dielectric permittivity with the temperature of the maximal dielectric constant increasing and the magnitude decreasing with increasing frequency. This behavior illustrates that PSMNT is a relaxor ferroelectric. It is noted that the peaks in Fig. 5(b) exhibit a more broad dispersive relaxation than those in Fig. 5(a), and the dielectric loss values in Fig. 5(b) are higher than those in Fig. 5(a), which suggest a higher level Pb-vacancies at the boule end where the ferroelectric phase is inhibited to develop up to a macroscopic scale and the system behaves with strong dielectric dispersion [14,15]. It is well known that the vapor pressure of PbO is high compared with that of the oxides of the B-site cationic species and that Pb loss occurs during the growth of the single crystals. This can be confirmed by a net weight loss 0.52% of the PSMNT powder. A small peak of the dielectric constant is observed near 70°C in Fig. 5(a), but there is no such small peak in Fig. 5(b), which indicates a rhombohedral or coexistence of the rhombohedral and tetragonal phases at the seed end of a boule, but only tetragonal phase exists at the end of the boule. The results are consistent with the XRD analysis. After poling, the permittivity  $\epsilon_{33}/\epsilon_0$  at room temperature varies from 3500

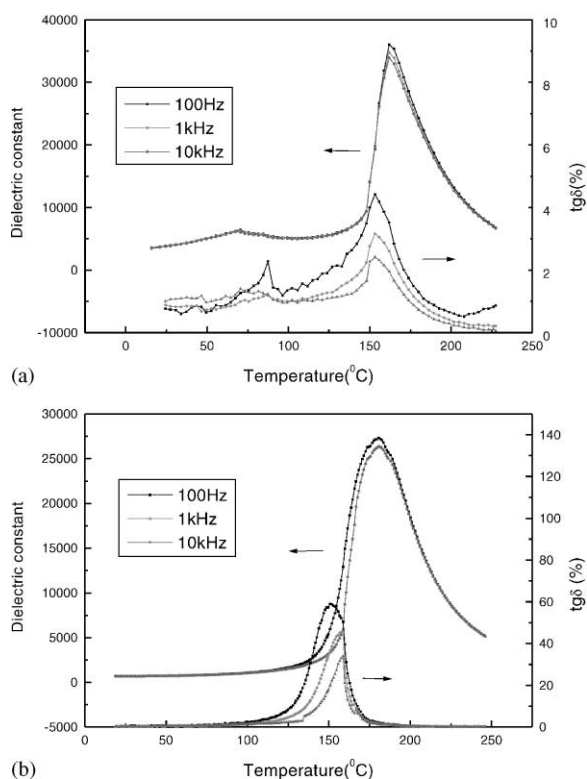


Fig. 5. Temperature frequency dependence of the dielectric constant and dielectric loss of poled plates cut from the seed end and boule end of the PSMNT5/62/32 single crystal shown in Fig. 3. (a) seed end (b) boule end.

to 700 for the two types of wafers in the same boule. The dielectric loss tangent,  $\text{tg}\delta$ , is lower than 1%.

For PSMNT plates cut from the seed end of a boule, the piezoelectric constant  $d_{33}$  is more than 1200 pC/N at room temperature, but the piezoelectric constant  $d_{33}$  is only about 400 pC/N for plates cut from the boule end. This can contribute to the domain engineering. The pseudorhombohedral spontaneous polarization orientations are aligned in the  $[111]_{\text{Cubic}}$  direction [8]. The high strain and associated piezoelectric properties are the result of the polarization orientation being field dependent and can be rotated towards a higher symmetry-tetragonal phase and to the applied field direction, i.e., polarization aligning parallel to the  $[001]_{\text{Cubic}}$  direction. They all have a large electromechanical coupling factor for the

thickness modes,  $k_t = 59.4\%$  and  $59.6\%$ , which is close to PMNT 67/33 single crystals. This also may portend a larger  $k_{33}$  value.

The modified Bridgman method was proved to be suitable for the growth of PSMNT single crystals. Further studies are in progress with a view to improving the homogeneity and to characterizing their piezoelectric properties along different axes. By optimizing the growth process and adjustment of the composition near the rhombohedral phase, we expect to obtain PSMNT single crystals near MPB of high quality and excellent piezoelectric performance for a wide range of electromechanical transducer applications.

#### 4. Conclusions

The ternary single crystals of PSMNT 5/63/32 have been successfully grown by a modified Bridgman technique. The crystals with perovskite phase were 15 mm in diameter and 20 mm in length. While PSMNT single crystals were grown near the MPB, the composition of a boule gradually changed from the range of rhombohedral phase at the seed end of a boule to tetragonal phase at the boule end. The dielectric properties of the plates cut from the seed end and the boule end of the same boule showed dielectric constant peaks of  $162^\circ\text{C}$  and  $180^\circ\text{C}$ , respectively, the room temperature permittivity also varied from 3500 to 700. The dielectric loss tangent,  $\text{tg}\delta$ , was lower than 1%. PSMNT cut from the seed end had the piezoelectric constant ( $d_{33}$ )  $\approx 1200$  pC/N, but the piezoelectric constant  $d_{33}$  of single crystals cut from boule end was only about 400 pC/N. They all had a larger  $k_t \approx 60\%$  for the thickness mode, which portended that PSMNT single crystals had great potential for application in ultrasonic transducers and high strain actuators.

#### Acknowledgements

This work was supported by the National Sciences Foundation of China (Grant Nos.

59995520, 59872048 and 50072038), the Shanghai Municipal Government (Grant No. 005207015)

## References

- [1] J. Kuwata, K. Uchino, S. Nomura, *Ferroelectrics* 37 (1981) 579.
- [2] S.-E. Park, T.R. Shrout, *IEEE Trans. Ultrason. Ferroelectron. & Freq. Control* 44 (1997) 1140.
- [3] J. Kuwata, K. Uchino, S. Nomura, *Jpn. J. Appl. Phys.* 21 (1982) 1298.
- [4] S.-E. Park, T.R. Shrout, *Mater. Res. Innovat.* 1 (1997) 20.
- [5] G. Xu, H. Luo, P. Wang, H. Xu, Z. Yin, *Chin. Sci. Bull.* (2000) 45.
- [6] K. Harada, S. Shimanuki, T. Kobayashi, S. Saitoh, Y. Yamsshita, *J. Am. Ceram. Soc.* 81 (1998) 2785.
- [7] K. Harada, S. Shimanuki, T. Kobayashi, S. Saitoh, Y. Yamsshita, *Key Eng. Mater.* (1999) 95.
- [8] Jianhua Yin, Wenwu Cao, *J. Appl. Phys.* 87 (2000) 7438.
- [9] S.-E. Park, T.R. Shrout, *J. Appl. Phys.* 82 (1997) 1804.
- [10] Yohachi Yamsshita, Kouichi Harada, *Jpn. J. Appl. Phys.* 36 (1997) 6039.
- [11] Y. Yamsshita, K. Harada, T. Tao, N. Ichinose, *Integr. Ferroelectron.* 13 (1996) 9.
- [12] Yasuharu Hosono, Kouichi Harada, Yohachi Yamsshita, Ming Dong, Z.G. Ye, *Jpn. J. Appl. Phys.* 39 (2000) 5589.
- [13] H. Luo, G. Xu, P. Wang, H. Xu, Z. Yin, *Jpn. J. Appl. Phys.* 39 (2000) 5581.
- [14] Z.-G. Ye, *Key Eng. Mater.* (1998) 81.
- [15] F. Chu, I.M. Reaney, N. Setter, *J. Appl. Phys.* 77 (1995) 1671.